再生しない内耳の機能を細胞移植により修復できる可能性を期待させる。ただし，内耳は非常に小さく，機能を損なうことなく細胞移植する方法を確立することに困難が予想される。内耳感覚器前駆細胞の障害内耳感覚器への移動効率や生存効率，感覚器細胞への分化効率を上昇させることができれば，障害内耳の機能を修復できる可能性があると思われる。また，現況ではヒト胎児の細胞を使用することは倫理的に困難である。ES細胞や自己由来の間葉系幹細胞などから内耳幹細胞が誘導できれば，細胞供給源の問題も解決できるであろう。

●文 献

1) Li H, Liu H, Heller S : Pluripotent stem cells from the adult mouse inner ear. Nat Med **9** : 1293-1299, 2003
2) Barald KF, Lindberg KH, Hardiman K, et al : Immortalized cell lines from embryonic avian and murine otocysts : tools for molecular studies of the developing inner ear. Int J Dev Neurosci **15** : 523-540, 1997
3) Holley MC, Nishida Y, Grix N : Conditional immortalization of hair cells from the inner ear. Int J Dev Neurosci **15** : 541-552, 1997
4) Rivolta MN, Grix N, Lawlor P, et al : Auditory hair cell precursors immortalized from the mammalian inner ear. Proc R Soc Lond B Biol Sci **265** : 1595-1603, 1998
5) Zheng JL, Lewis AK, Gao WQ : Establishment of conditionally immortalized rat utricular epithelial cell lines using a retrovirus-mediated gene transfer technique. Hear Res **117** : 13-23, 1998
6) Kalinec F, Kalinec G, Boukhvalova M, et al : Establishment and characterization of conditionally immortalized organ of corti cell lines. Cell Biol Int **23** : 175-184, 1999
7) Lawlor P, Marcotti W, Rivolta MN, et al : Differentiation of mammalian vestibular hair cells from conditionally immortal, postnatal supporting cells. J Neurosci **19** : 9445-9458, 1999
8) Rivolta M, Holley MC : Asymmetric segregation of mitochondria and mortalin correlates with the multi-lineage potential of inner ear sensory cell progenitors *in vitro*. Brain Res Dev Brain Res **133** : 49-56, 2002
9) Sher AE : The embryonic and postnatal development of the inner ear of the mouse. Acta Oto-Laryngol **285** : 1-77, 1971
10) Fekete DM, Muthukumar S, Karagogeos D : Hair cells and supporting cells share a common progenitor in the avian inner ear. J Neurosci **18** : 7811-7821, 1998
11) Lang H, Fekete DM : Lineage analysis in the chicken inner ear shows differences in clonal dispersion for epithelial, neuronal, and mesenchymal cells. Dev Biol **234** : 120-137, 2001
12) Malgrange B, Belachew S, Thiry M, et al : Proliferative generation of mammalian auditory hair cells in culture. Mech Dev **112** : 79-88, 2002
13) Zhao HB : Long-term natural culture of cochlear sensory epithelia of guinea pigs. Neurosci Lett **315** : 73-76, 2001
14) Kojima K, Murakami S, Ito J : Establishment of dissociated culture system of inner ear sensory epithelial cells. Otology Japan **11** : 175-178, 2001
15) Kim TS, Kojima K, Nishida AT, et al : Expression of calretinin by fetal otocyst cells after transplantation into damaged rat utricle explants. Acta Otolaryngol Suppl : 34-38, 2004
16) Gage FH, Coates PW, Palmer TD, et al : Survival and differentiation of adult neuronal progenitor cells transplanted to the adult brain. Proc Natl Acad Sci USA **92** : 11879-11883, 1995
17) Takahashi M, Palmer TD, Takahashi J, et al : Widespread integration and survival of adult-derived neural progenitor cells in the developing optic retina. Mol Cell Neurosci **12** : 340-348, 1998
18) Nishida A, Takahashi M, Tanihara H, et al : Incorporation and differentiation of hippocampus-derived neural stem cells transplanted in injured adult rat retina. Invest Ophthalmol Vis Sci **41** : 4268-4274, 2000

難聴の最新研究

再生医学

細胞移植で機能回復をめざす

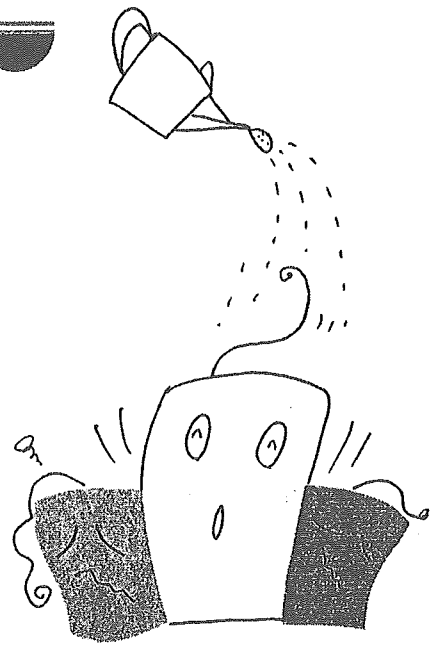

京都大学大学院医学研究科
耳鼻咽喉科・頭頸部外科
特任助手（COE研究院）
小島 憲

同教授
伊藤壽一

人工臓器、臓器移植の限界を克服

細胞レベルで体を元どおりにする「再生医学」

事故や病気などにより体の一部が失われたり、うまく機能しなくなったりすることがあります。障害の程度がわれわれ自身の治癒力を超えてしまえば、失われた体を元どおりに取り戻すことはできません。このような場合には、失ってしまった体の機能を取り戻すためにさまざまな試みがなされています。すでに一部の臓器ではその機能を人工器官に置き換える、または臓器移植を行って失われた機能を再獲得する、などのことが行われています。たとえば人工透析や腎移植・肝移植・心臓移植などです。耳鼻咽喉科領域では高度難聴に対して人工内耳が用いられるようになってきました。しかしながら人工臓器で機能を完全に修復することはいまのところ困難であり、臓器移植もドナーの不足や拒絶反応、倫理的問題などさまざまな問題をかかえ、いまだに決め手にかけるのが現状です。

人工臓器や臓器移植の限界を超えるため、細胞レベルでいろいろな工夫を凝らし、障害を被ってしまった体を元どおりに、すなわち再生させることをめざしたのが「再生医学」です。現在では体の組織のすべてが再生医学のターゲットになっているといっても過言ではありません。

内耳再生のターゲットは5つの細胞

細胞移植は再生医学の切り札的存在

内耳領域における再生医学のターゲットを図1に挙げます。

障害組織にそのもとになる細胞（幹細胞・前駆細胞）が残っていれば、それらの細胞を増や

図1　内耳再生医学の対象とされている細胞

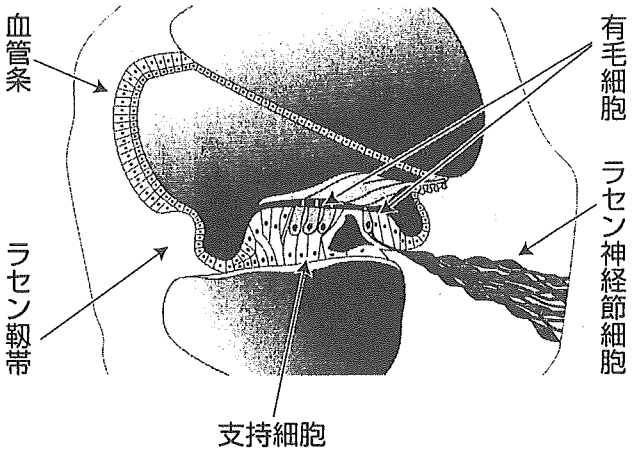

剤投与や遺伝子導入によりこの細胞の増殖を刺激してあらたな有毛細胞や神経節細胞をつくる可能性が示されました。不可能と考えられていた内耳の再生に大きく踏み出す一歩といえます。

しかし組織が高度に傷害された場合、ただでさえ少ない内在性の幹細胞を利用できるとは限りません。このようなケースでは外から細胞を入れる必要があります。すなわち「細胞移植」です。

臨床の現場でもっとも頻繁に行われている細胞移植は、白血病治療の際に行われる骨髄移植でしょう。今日では骨髄移植以外にも末梢血造血幹細胞移植や臍帯血移植なども行われています。骨髄移植の臨床応用は拒絶反応の制御技術の向上など医学的な問題だけでなくドナー確保のための移植バンクやネットワークの形成、法律の整備など社会的にもさまざまな進展をもたらしました。

最新の成果として挙げられるのは1型糖尿病患者への膵島（膵ランゲルハンス島）移植の臨床応用です。2004年4月に国内初の膵島移植が、2005年1月には世界初の生体膵島移植が京都大学医学部附属病院で行われました。膵島移植は、純化した膵島細胞を移植するので膵臓移植の際に起こる外分泌組織による合併症を回避できます。また、門脈から点滴を用いて肝臓内に移植するので大きな手術侵襲を伴いません。拒絶反応が膵島移植のほうが軽いなどの利点もあり、今後の普及が期待されています。

しかしながら臓器移植同様、細胞移植もドナー不足は深刻です。そこで注目されているのが旺盛な増殖能を持つ、いわゆる幹細胞です。

さまざまな細胞に分化する「幹細胞」

○●●○胚性幹細胞と組織幹細胞に大別され、旺盛な増殖能をもつ

幹細胞は、胚性幹細胞（ES細胞）と組織幹細胞に大別できます。ES細胞は、受精後5～6日目の胚盤胞からとりだされる細胞で、非常に旺盛な増殖能を持つとともに体のすべての細胞に分化する能力（多能性）を持つといわれています。韓国とアメリカの研究グループは実際に疾患を持つ患者の核を移植して作製したクローン胚からES細胞を効率よく作ることに成功しました。

また、つい最近ですがアメリカのハーバード大学のグループは、成人の皮膚の細胞をES細胞と融合させてES細胞様の性質を持たせることにも成功しています。このようにして作られた細胞から目的の細胞を作り出

すことができれば移植に十分な数の細胞を得ることができると同時に、細胞を移植した後も拒絶反応が起こりにくいと予想されています。

一方の組織幹細胞は自己複製能を持ち、所属する組織のすべての種類の細胞に分化する能力（多分化能）を持つ細胞と定義されています。なかでも骨髄に存在する「間葉系幹細胞」はES細胞のように分化の可塑性が高いと考えられており、神経や筋肉、血管などさまざまな細胞になると報告されています。2005年夏には、心筋梗塞の患者さんに骨髄から得た細胞を移植することにより、良好な結果を得たとの発表が日本でもありました。慢性閉塞性血管障害や脊髄損傷に対して間葉系幹細胞移植を行う計画もなされています。そのメカニズムや有効性はまだ明らかではありませんが、患者さん本人の骨髄を使うことができれば、拒絶反応やドナーの問題だけでなく、臓器移植やES細胞移植が直面する倫理的な問題をも回避できると期待されています。

再生医学で感音難聴を治すための試み

- 有毛細胞の再生だけでは難聴の回復は困難。遺伝子導入や薬剤投与などの組み合わせが必要

前述のように、大人の内耳にも有毛細胞になることのできる幹細胞・前駆細胞が存在する可能性が示されています。しかし、障害が強い場合や慢性期になってからでは有毛細胞前駆細胞が残存しているとは考えにくく、このような場合は有毛細胞の前駆細胞を補う、すなわち幹細胞移植が必要になると考えています。これまでに、神経幹細胞やES細胞、骨髄細胞を用いて内耳細胞移植療法の可能性を示しました（図2）。しかしながら、有毛細胞のみ再生させても難聴を回復させることはできません。なぜなら、強い内耳障害の場合、信号の伝達に必須なラセン神経節や、有毛細胞が機能するための環境を整える血管条やラセン靱帯、支持細胞も傷害されるからです。ラセン神経節や靱帯に対してもES細胞や間葉系幹細胞を移植する試みが行われています。現在のところ移植細胞の生着率は低く、また、内耳に安全に細胞を導入する方法も確立していません。しかし、近いうちにこのような問題は解決されることでしょう。また、将来的には細胞移植だけでなく、遺伝子導入や薬剤投与などを組み合わせることにより、高度感音難聴が治療される時代がくると確信しています。

図2　新生仔ラット内耳に移植した神経幹細胞

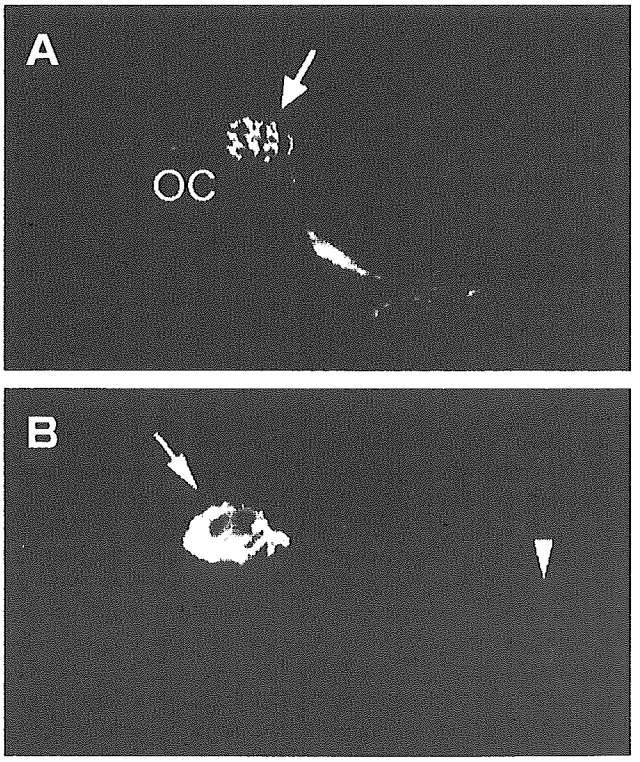

移植神経幹細胞（矢印）はコルチ器内に生着し（A）、有毛細胞のマーカーの1つであるファロイジン（矢印）を発現する細胞も存在した（B）。▼はファロイジン強陽性細胞（感覚上皮内に入っている）
（Acta Otolaryngol 121:140-142.より引用）

The Laryngoscope
Lippincott Williams & Wilkins, Inc.

Novel Strategy for Treatment of Inner Ears using a Biodegradable Gel

Tsuyoshi Endo, MD; Takayuki Nakagawa, MD, PhD; Tomoko Kita, PhD; Fukuichiro Iguchi, MD, PhD; Tae-Soo Kim, MD, PhD; Tetsuya Tamura, MD; Koji Iwai, MD; Yasuhiko Tabata, PhD; Juichi Ito, MD, PhD

Objective: **The present study aimed to evaluate the efficacy of a biodegradable hydrogel as a drug-delivery medium for the inner ear. Brain-derived neurotrophic factor (BDNF) was chosen as the agent to be administered.** ***Method:*** **First, we used an enzyme-linked immunosorbent assay to measure BDNF concentrations in the cochlear fluid after placing a hydrogel containing this agent onto the round-window membrane of the ear. Second, the functional and histologic protection of the auditory primary neurons (spiral ganglion neurons [SGNs]) by BDNF applied through the hydrogel was examined using an animal model of SGN degeneration.** ***Results:*** **The results revealed sustained delivery of BDNF into the cochlear fluid by way of the hydrogel. Second, the functional and histologic protection of the auditory primary neurons (SGNs) by BDNF applied through the hydrogel was examined using an animal model of SGN degeneration. The measurement of electrically evoked auditory-brainstem responses demonstrated that BDNF delivered by way of the hydrogel significantly reduced the threshold elevation. Immunohistochemistry for neurofilament 200 kD demonstrated increased survival of SGNs because of BDNF application through the hydrogel.** ***Conclusion:*** **These findings indicate that biodegradable hydrogels can be used for drug delivery to the inner ear.** ***Key Words:*** **Drug delivery, HL, inner ear, neurotrophins, protection.**

Laryngoscope, **115:2016–2020, 2005**

From the Department of Otolaryngology–Head and Neck Surgery, Graduate School of Medicine (T.E., T.N., T.K., T.-S.K., T.T., K.I., J.I.), the Institute for Frontier Medical Science (Y.T.), Kyoto University, Kyoto, Japan, and the Department of Otolaryngology, Otsu Red Cross Hospital (F.I.), Otsu, Japan.

Editor's Note: This manuscript was accepted for publication August 10, 2005.

This study was supported by a Grant-in-Aid for Regenerative Medicine Realization from the Ministry of Education, Science, Sports, Culture and Technology of Japan.

A part of this study was presented at the 40th Workshop on Inner Ear Biology, Granada, Spain, September 8–10, 2003 and the 27th Midwinter meeting for the Association for Research in Otolaryngology, Daytona Beach, Florida, U.S.A., February 21–26, 2004.

Send Correspondence to Dr. Takayuki Nakagawa, Department of Otolaryngology–Head and Neck Surgery, Graduate School of Medicine, Kyoto University, Kawaharacho 54, Shogoin, Sakyo-ku, 606-8507 Kyoto, Japan. E-mail: tnakagawa@ent.kuhp.kyoto-u.ac.jp

DOI: 10.1097/01.mlg.0000183020.32435.59

INTRODUCTION

Sensorineural hearing loss (SNHL) is one of the most common disabilities in industrial countries. However, therapeutic strategies for the treatment of SNHL are limited to hearing aids and cochlear implants. Excessive noise, ototoxic drugs, genetic disorders, and aging can all cause SNHL. Previous studies on human temporal bones and animal models have indicated that the loss of cochlear hair cells and cochlear neurons (spiral ganglion neurons [SGNs]) are among the major causes of SNHL.[1] Loss of auditory function caused by the degeneration of auditory hair cells can be partly restored by cochlear implants, which are small devices that are surgically implanted into the inner ear to stimulate SGNs. However, the success of these implants depends on the remaining SGNs, and their loss severely compromises the efficacy of this technique.[2] Protecting these cells from irreversible degeneration is therefore of primary importance.

The problem of how to deliver drugs to the inner ear has been a considerable obstacle to the development of treatments for inner ear degeneration. The systemic application of drugs carries the risk of unwanted side effects. In addition, the blood–inner ear barrier, which inhibits the transport of drugs from the serum to the inner ear, represents a fundamental obstacle to systemic application.[3] The inner ear tissues are isolated from the surrounding organs by a bony construction, which allows the topical introduction of drugs by local application. On the basis of these considerations, local application has generally been used for drug application to the inner ear. The inner ear is connected to the middle ear cavity by the round-window membrane (RWM). Drug application through the RWM has therefore been exploited as a route for the local application of drugs to the inner ear; this approach has been reported for the clinical application of both steroids[4] and gentamicin.[5] However, this technique has not been widely used in a clinical setting because controlled, noninvasive delivery systems have not yet been developed.

A biodegradable hydrogel has been developed for the sustained delivery of proteins, including growth and trophic factors.[6–8] In this approach, a positively charged protein is electrostatically complexed with negatively charged polymer chains, which are components of the

biodegradable hydrogel. Biodegradation of the polymer chains leads to release of the protein, which is regulated by changes that occur during the degradation process. The efficacy of this drug-delivery system has been demonstrated for the release of basic fibroblast growth factor for angiogenesis[7] and bone morphogenetic protein 1 for bone formation.[8]

In the present study, we examined whether biodegradable hydrogels could be used for the sustained delivery of brain-derived neurotrophic factor (BDNF), which is known to promote the survival of SGNs,[9,10] to the inner ear by way of the RWM.

MATERIALS AND METHODS

Experimental Animals

Pigmented guinea pigs weighing 250 to 300 g were purchased from Japan SLC, Inc., (Hamamatsu, Japan) for use in this study. Animal care was carried out under the supervision of the Institute of Laboratory Animals of the Graduate School of Medicine, Kyoto University, Japan.

Biodegradable Hydrogels

Biodegradable hydrogels were prepared as described previously.[6–8] They were generated through the glutaraldehyde cross-linking of porcine type-I collagen (Gunze, Ayabe, Japan). The rates of degradation were determined according to the concentration of glutaraldehyde. We used the hydrogel generated with 60 0mol/L glutaraldehyde in this study.

BDNF Concentrations in Perilymph

Pigmented guinea pigs were anesthetized with ketamine (20 mg/kg, intramuscularly [IM]; Sankyo Co., Tokyo, Japan) and xylazine (5 mg/kg, IM; Bayer, Tokyo, Japan). A hydrogel immersed with BDNF (84 μg dissolved in 2 μL physiologic saline) was positioned on the RWM of each animal in the treated group (n = 20). For animals in the control group (SAL, n = 20), a hydrogel immersed with physiologic saline alone was placed on the RWM. Finally, animals in the injection group (n = 20) received an injection of BDNF (84 μg dissolved in 2 μL physiologic saline) through the RWM. The perilymph was collected on day 3 or 7 after the drug application to measure the BDNF concentration. For each animal, a small hole was made in the basal turn of the cochlea 2 mm from the RWN, under general anesthesia, and 2 μL of the perilymph was collected through the hole using a micropipette. BDNF proteins in the perilymph (10 μL from 5 animals) were quantified using an enzyme-linked immunoadsorbent assay (ELISA). The ELISA was performed using a BDNF Emax Immunoassay System kit according to standard protocols (Promega, Madison, WI). The triplicates were averaged, and the values were corrected for the total amount of protein in the sample. Values for BDNF protein levels were expressed as pg/mg of total protein.

Functional Protection

An animal model of the degeneration of SGNs[10,11] was used to evaluate the functional and morphologic protection of SGNs induced by the application of BDNF through a biodegradable hydrogel. The functionality of the cochleae was assessed using the electrically evoked auditory brain-stem response (eABR). Pigmented guinea pigs received an IM injection of kanamycin (KM; 400 mg/kg; Wako Pure Chemical Industries, Ltd., Osaka, Japan) and an intravenous injection of ethacrynic acid (EA; 25 mg/kg; Wako Pure Chemical Industrie,s Ltd) to induce the total loss of cochlear hair cells, resulting in the secondary degeneration of SGNs. On day 18, after the KM and EA treatment, the eABR thresholds were measured in four animals without drug application. For animals in the SAL group, a hydrogel immersed with 2 μL physiologic saline was positioned on the RWM on day 18 (n = 12). In the BDNF group, a hydrogel immersed in BDNF (84 μg dissolved in 2 μL physiologic saline) was placed on the RWM of each animal (n = 12). Measurement of the eABR thresholds was performed 3 or 7 days after drug application (n = 4 in each case) using the method described by Hall.[12] The eABRs typically demonstrated a classic waveform consisting of five positive waves, and thresholds were determined using wave III. The threshold was defined as the lowest stimulus level in 50 μA steps that evoked a replicable waveform.

Histologic Protection

Histologic protection was evaluated on the basis of the cell densities of surviving SGNs in the Rosenthal's canals. On day 7 after drug application, the animals were deeply anesthetized with a lethal dose of ketamine and xylazine and were perfused intracardially with physiologic saline followed by 4% paraformaldehyde in 0.01 mol/L phosphate-buffered saline at pH 7.4. Four temporal bones were collected from each experimental group and immersed in the same fixative at 4°C for 12 hours. Specimens were prepared as cryostat sections (thickness 10 μm) after decalcification with 0.1 mol/L ethylenediamine tetra-acetic acid for 14 days at 4°C. Four mid-modiolus sections were chosen from each cochlea and stained by immunohistochemistry for neurofilament (NF) 200 kD and peripherin: the former was used as a marker for neurons and the latter as a marker for type II SGNs.[13] Anti-NF mouse monoclonal antibody (1:500; Sigma, St. Louis, MO) and antiperipherin rabbit polyclonal antibody (1:200; Chemicon, Temecula, CA) were used as primary antibodies. Fluorescein isothiocyanate-conjugated antimouse goat antibody (1:400; Santa Cruz Biotechnology, Santa Cruz, CA) and rhodamine-conjugated antirabbit donkey antibody (1:500; Chemicon) were used as secondary antibodies. Counterstaining by DAPI (Molecular Probes, Eugene, OR) was performed at the end of the staining procedures. Nonspecific labeling was tested by omitting the primary antibody from the staining procedures. The specimens were viewed with a Nikon ECLIPSE E600 fluorescence microscope (Nikon, Tokyo, Japan). Both NF- and DAPI-positive cells located in the Rosenthal's canal were defined as SGNs, and peripherin-positive cells were regarded as type II SGNs. The numbers of SGNs and type II SGNs were counted in each turn of the cochleae. The area of the Rosenthal's canal was measured on bright-field images using NIH image software (version 1.62; http://rsb.info.nih.gov/nih-image). The density of SGNs and type II SGNs was then calculated. The average of the densities from four sections was defined as the data point for each animal.

Statistical Analyses

Two-factor factorial analysis of variance was used to determine the statistical significance differences between the BDNF concentrations in the perilymph and the eABR thresholds among the experimental groups. A pair-wise comparison was performed using multiple comparisons with the Tukey-Kramer test. Differences in SGN or type II SGN densities in each turn of the cochleae among the experimental groups were examined using unpaired t tests. For all analyses, a probability (P) value less than .01 was considered to be statistically significant. Values are expressed as mean ± SD.

RESULTS

BDNF Concentrations in Perilymph

The BDNF concentrations in the perilymph of the SAL and injection groups were either extremely low or

undetectable: the values (pg/mL) were 3.39 ± 4.70 on day 3 after treatment and 2.77 ± 3.30 on day 7 for the SAL group and 16.39 ± 5.83 on day 3 and 8.26 ± 2.23 on day 7 for the injection group. The hydrogel group exhibited apparently higher concentrations of BDNF on days 3 and 7 compared with the other experimental groups: the values were 675.00 ± 230.22 on day 3 and 884.77 ± 100.35 on day 7 (Fig. 1). The overall effect of the experimental groups on BDNF concentrations were statistically significant ($P < .0001$). Significant differences were also detected in the BDNF concentrations on days 3 and 7 between the SAL and gel groups and between the injection and gel groups.

Functional Protection

The eABR threshold on day 18 after KM and EA treatment (before drug application) was 0.727 ± 0.092 mA. The SAL group exhibited an obvious elevation of the eABR threshold over time: the values (mA) were 0.960 ± 0.079 on day 3 and 0.992 ± 0.073 on day 7 (Fig. 2). By contrast, no significant elevation of the threshold was detected in the BDNF group: the values were 0.745 ± 0.067 on day 3 and 0.760 ± 0.073 on day 7 (Fig. 2). The overall effect of the experimental groups on elevation of the eABR threshold was statistically significant ($P < .0001$). Significant differences were also detected in the thresholds on day 3 or 7 between the SAL and BDNF groups. The thresholds of the SAL group on days 3 and 7 were significantly higher than those before drug application, whereas no significant differences were detected after BDNF application. These findings indicate that the application of BDNF by way of the biodegradable hydrogel maintained the functionality of the SGNs.

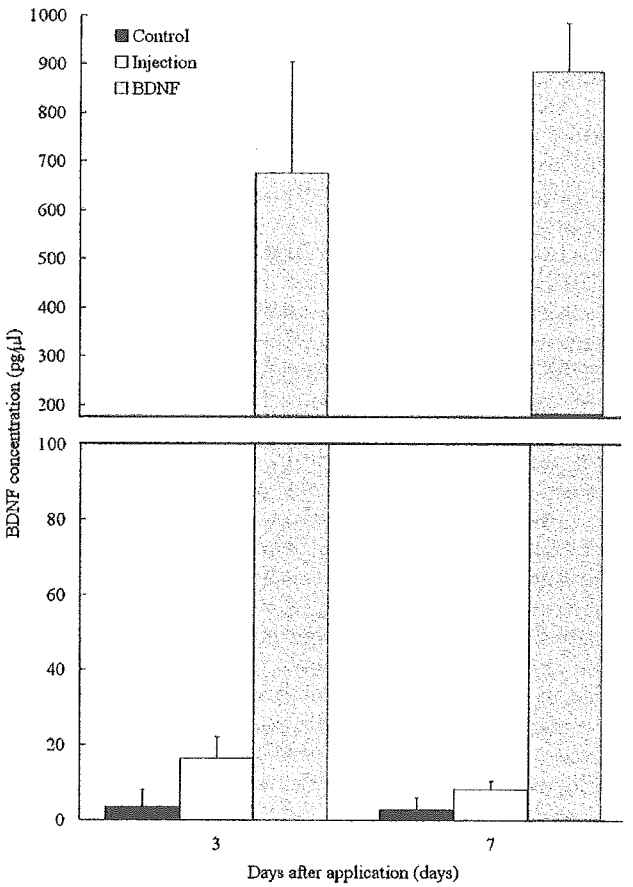

Fig. 1. Brain-derived neurotrophic factor (BDNF) concentrations in the perilymph 3 or 7 days after BDNF application by hydrogel, single injection, or no treatment. Bars on left show BDNF concentrations in the perilymph without treatment (control group), those in the middle values after a single injection (injection group), and those on the right results of the hydrogel application (gel group). Significant differences in BDNF concentrations in the perilymph were detected between the control and gel groups and the injection and gel groups. *Multiple comparisons with the Tukey–Kramer test. Bars represent SDs.

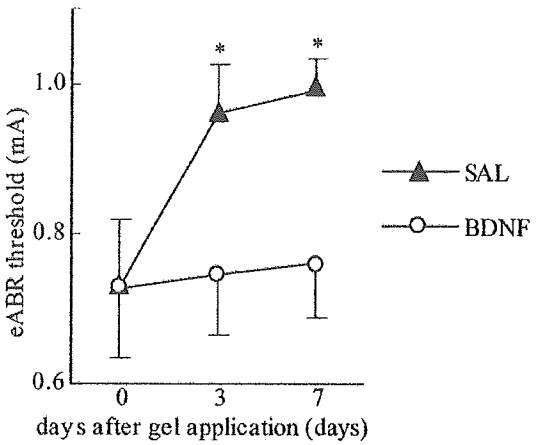

Fig. 2. Functional assessment of the protective effects of brain-derived neurotrophic factor (BDNF) applied by way of a hydrogel against the consecutive degeneration of spiral ganglion neurons (SGN) after hair cell loss. Evoked auditory brain-stem response (eABR) thresholds 0, 3, and 7 days after BDNF application (BDNF) by way of the hydrogel (open circles). eABR thresholds 0, 3, or 7 days after physiologic saline application by way of the hydrogel (control group [SAL]) (closed triangles). Significant differences in the eABR thresholds were detected between the BDNF and SAL groups 3 or 7 days after application. *Multiple comparisons with the Tukey–Kramer test. Bars represent SDs.

Histologic Protection

Immunohistochemistry for NF confirmed the lack of degeneration of SGNs in the cochleae before drug application: the densities (cells/10,000 μm^2) were 25.66 ± 3.26 for the basal turn, 23.77 ± 4.37 for the second turn, and 19.64 ± 3.02 for the third turn. The densities of type II SGNs before drug application were 0.76 ± 0.31 for the basal turn, 0.65 ± 0.52 for the second turn, and 0.71 ± 0.47 for the third turn. Severe degeneration of the SGNs was observed in the SAL group (Fig. 3, D, E, and F) and was apparent in the basal portion of the cochleae: the densities were 3.46 ± 0.88 for the basal turn, 6.52 ± 2.95 for the second turn, and 7.19 ± 3.47 for the third turn. By contrast, no significant degeneration of type II SGNs was observed in the cochleae of the SAL group (Fig. 3, D, E, and F): the densities were 0.73 ± 0.68 for the basal turn, 0.53 ± 0.77 for the second turn, and 0.99 ± 0.38 for the third turn. Although degeneration of the SGNs was detected in the BDNF group, it was limited in comparison with that observed in the SAL group (Fig. 3, A, B, and C):

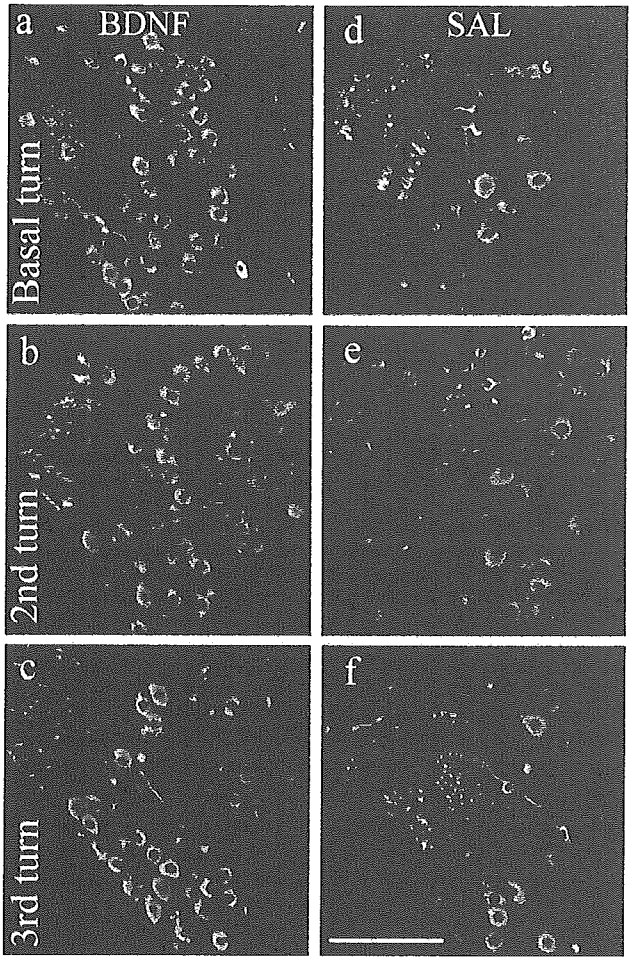

Fig. 3. Immunohistologic evaluation of degeneration of the spiral ganglion neurons (SGN) in each turn of the cochleae 7 days after treatment with a hydrogel immersed with brain-derived neurotrophic factor (BDNF) solution or physiologic saline alone. Immunohistochemistry for neurofilament 200 kD reveals neurons in the Rosenthal's canal (red), whereas immunohistochemistry for peripherin labels type II SGNs (green). Images of SGNs treated with BDNF solutions (BDNF; A to C). SGNs treated with physiologic saline alone (SAL; D to F). Degeneration of the SGNs is apparent in the SAL specimens compared with the BDNF specimens, whereas no significant differences are visible in type II SGNs. Scale bar = 50 μm.

the densities were 11.35 ± 2.77 for the basal turn, 17.97 ± 4.69 for the second turn, and 26.61 ± 8.44 for the third turn. The differences in SGN densities between the BDNF and SAL groups were significant for each turn of the cochleae ($P < .001$) (Fig. 4). No apparent degeneration of the type II SGNs was observed in the BDNF group: the densities were 0.77 ± 0.92 for the basal turn, 0.89 ± 0.93 for the second turn, and 1.09 ± 0.98 for the third turn. No significant differences were observed between the two experimental groups in the densities of type II SGNs in each turn of the cochleae. These findings indicate that type I SGNs are predominantly degenerated in this model and that BDNF application by way of the hydrogel promotes their survival.

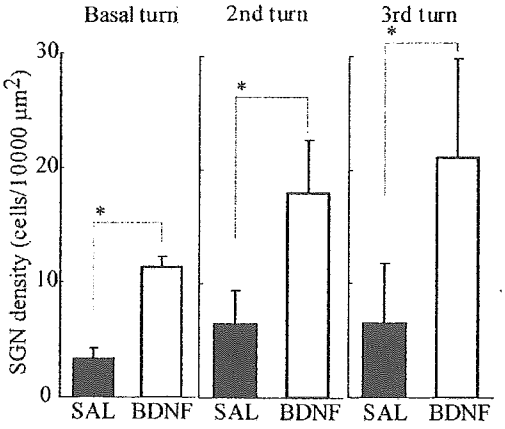

Fig. 4. Densities of spiral ganglion neurons (SGN) in each turn of the cochleae treated with brain-derived neurotrophic factor (BDNF) solution or physiologic saline. Densities of SGNs in cochleae administered BDNF solution after ototoxic treatment (BDNF; bars on right). Densities of SGNs in cochleae administered physiologic saline after ototoxic treatment (SAL; bars on left). *$P < .001$; unpaired t test. Bars represent SDs.

DISCUSSION

Our findings demonstrate the efficient transfer of BDNF into the inner ear using a biodegradable hydrogel. This indicates that the placement of a biodegradable hydrogel on the RWM is an effective method for the local application of neurotrophins to the inner ear. ELISA analyses in the present study confirmed the sustained delivery of BDNF to the cochlear fluid for 7 days by way of the biodegradable hydrogel. In addition, the functional and morphologic protection of SGNs was observed 7 days after BDNF application, indicating that its biological effects were maintained during this period. Biodegradable hydrogels can be injected through the tympanic membrane, and this relatively straightforward procedure can be performed at outpatient clinics by general otolaryngologists.

Previous studies investigating the efficacy of neurotrophins against inner ear degeneration have used the implantation of an osmotic minipump[9,14] or gene transfer by virus vectors[10,15] as drug-application methods. The osmotic minipump is implanted into the subcutaneous tissue, and a tube from the pump is inserted into the basal turn of the cochlea. This method can provide the stable transfer of neurotrophins into the cochlear fluid, resulting in the successful protection of SGNs.[9,14] The use of osmotic minipumps requires middle and inner ear surgery, whereas that of hydrogels only involves positioning the hydrogel on the RWM. Gene transfer using adeno or adeno-associated vectors is an established method for introducing genes of neurotrphins into the inner ear.[10,15] Although recent studies using virus vectors have shown no significant toxicity, this risk remains a major problem in clinical applications. In contrast with virus vectors, biodegradable hydrogels are made from porcine collagen and have no toxity.[6–8] We, therefore, consider the biodegradable hydrogel to be better suited for clinical use than the osmotic minipump or gene transfer.

CONCLUSION

Efforts to reduce degeneration in the inner ear have identified several agents for the protection of hair cells or SGNs. Among these are trophic factors, several of which are commercially available for clinical use. Previous experimental studies have confirmed the protective effects of trophic factors for the inner ear. In the current study, we chose to apply BDNF because its protective effect on SGNs has been verified in several studies using diverse methods. However, biodegradable hydrogels could be used for the delivery of a number of other trophic factors. We believe that our findings will help to advance the clinical application of trophic factors for the treatment of inner ear diseases.

Acknowledgments

The authors thank Norio Yamamoto for generously supporting us with ELISA, Rika Sadato for technical assistant of histologic analysis, and Toshihiro Kushibiki for making the hydrogel.

BIBLIOGRAPHY

1. Nordmann AS, Bohne BA, Harding GW. Histopathological differences between temporaryand permanent threshold shift. *Hear Res* 2000;139:13–30.
2. Nadol JJ, Young YS, Glynn RJ. Survival of spiral ganglion cells in profound sensorineural hearing loss: implications for cochlear implantation. *Ann Otol Rhinol Laryngol* 1989; 98:411–416.
3. Juhn SK, Rybak LP. Labyrinthine barriers and cochlear homeostasis. *Acta Otolaryngol* 1981;91:529–534.
4. Lefebvre PP, Staecker H. Steroid perfusion of the inner ear for sudden sensorineural hearing loss after failure of conventional therapy: a pilot study. *Acta Otolaryngol* 2002; 122:698–702.
5. Minor LB, Schessel DA, Carey JP. Meniere's disease. *Curr Opin Neurol* 2004;17:9–16.
6. Tabata Y, Ikada Y. Controlled release of vascular endothelial growth factor by use of collagen hydrogels. *J Biomater Sci Polym Ed* 2000;11:915–930.
7. Iwakura A, Fujita M, Kataoka K, et al.Intramyocardial sustained delivery of basic fibroblast growth factor improves angiogenesis and ventricular function in a rat infarct model. *Heart Vessels* 2003;18:93–99.
8. Yamamoto M, Takahashi Y, Tabata Y. Controlled release by biodegradable hydrogels enhances the ectopic bone formation of bone morphogenetic protein. *Biomaterials* 2003;24: 4375–4383.
9. Shinohara T, Bredberg G, Ulfendahl M, et al.Neurotrophic factor intervention restores auditory function in deafened animals. *Proc Natl Acad Sci U S A* 2002;99:1657–1660.
10. Nakaizumi T, Kawamoto K, Minoda R, et al. Adenovirus-mediated expression of brain-derived neurotrophic factor protects SGNs from ototoxic damage. *Neurootology* 2004;9: 135–143.
11. West BA, Brummett RE, Himes DL. Interaction of kanamycin and ethacrynic acid. Severe cochlear damage in guinea pigs. *Arch Otolaryngol* 1973;98:32–37.
12. Hall RD. Estimation of surviving spiral ganglion cells in the deaf rat using the electrically evoked auditory brainstem response. *Hear Res* 1990;49:155–168.
13. Mou K, Hunsberger CL, Cleary JM, et al. Synergistic effects of BDNF and NT-3 on postnatal spiral ganglion neurons. *J Comp Neurol* 1997;386:529–539.
14. Ylikoski J, Pirvola U, Suvanto J, et al. Guinea pig auditory neurons are protected by glial cell line-derived neurotrophic factor from degeneration after noise trauma. *Hear Res* 1998;124:17–26.
15. Yagi M, Magal E, Sheng Z, et al .Hair cell protection from aminoglycoside ototoxicity by adenovirus-mediated overexpression of glial cell line-derived neurotrophic factor. *Hum Gene Ther* 1999;10:813–823.

Available online at www.sciencedirect.com
SCIENCE DIRECT®
Hearing Research 205 (2005) 201–209
HEARING RESEARCH
www.elsevier.com/locate/heares

Disruption and restoration of cell–cell junctions in mouse vestibular epithelia following aminoglycoside treatment

Tae-Soo Kim [a], Takayuki Nakagawa [a,*], Shin-ichiro Kitajiri [a,b,d], Tsuyoshi Endo [a], Shinji Takebayashi [a], Fukuichiro Iguchi [a], Tomoko Kita [a,c], Tetsuya Tamura [a], Juichi Ito [a]

[a] *Department of Otolaryngology-Head and Neck Surgery, Graduate School of Medicine, Kyoto University, Kawaharacho 54, Shogoin, Sakyo-ku, 606-8507 Kyoto, Japan*
[b] *Department of Cell Biology, Graduate School of Medicine, Kyoto University, Kawaharacho 54, Shogoin, Sakyo-ku, 606-8507 Kyoto, Japan*
[c] *Horizontal Medical Research Organization, Graduate School of Medicine, Kyoto University, Kawaharacho 54, Shogoin, Sakyo-ku, 606-8507 Kyoto, Japan*
[d] *Solution Oriented Research for Science and Technology, Japan Science and Technology Corporation, 54 Kawahara-cho, Shogoin, Sakyo-ku, Kyoto 606-8507, Japan*

Received 2 September 2004; accepted 18 March 2005
Available online 20 April 2005

Abstract

The intracellular junction complexes, which consist of tight junctions (TJ), adherens junctions (AJ), and desmosomes, mediate cell–cell adhesion in epithelial cells. E-cadherin, which is a major component of AJ, plays a role not only in the maintenance of cell–cell junctions, but also in repressing cell proliferation. In this study, we examined changes of E-cadherin expression in mouse vestibular epithelia following local application of neomycin using immunohistochemistry and western blotting, and morphology of cell–cell junctions by transmission electron microscopy (TEM). Immunohistochemistry and western blotting revealed down-expression of E-cadherin and its consecutive recovery. TEM demonstrated temporal disruption of cell–cell junctions. Morphology of cell–cell junctions was more rapidly restored than recovery of E-cadherin expression. Transient disruption of cell–cell junctions and down-expression of E-cadherin is a rational response for the deletion of dying hair cells, and may be associated with a limited capacity for cell proliferations in mammalian vestibular epithelia following their rapid restoration.

Keywords: Inner ear; Adherens junction; Tight junction; Aminoglycoside ototoxicity; E-cadherin

1. Introduction

The intracellular junctional complexes of epithelial cells consist of three components: tight junctions (TJ), adherens junctions (AJ), and desmosomes (Farquhar and Palade, 1963). E-cadherin is an extracellular calcium-dependent transmembrane adhesion molecule that mediates cell–cell interaction through AJ between epithelial cells (Takeichi, 1991). Classic cadherin molecules in AJ are transmembrane homophilic adhesion receptors that indirectly associate with the actin cytoskeleton by interacting with catenins (Tsukita et al., 1992). E-cadherin plays a role not only in the maintenance of cell–cell junctions, but also in the regulation of cell proliferation, migration, and differentiation (Gumbiner et al., 1988; Birchmeier and Behrens, 1994; Vleminckx and Kemler, 1999).

Abbreviations: TJ, tight junction(s); AJ, adherens junction(s); NM, neomycin; TEM, transmission electron microscopy; SC, supporting cell(s); HC, hair cell(s); PSCC, posterior semicircular canal ducts; PBS, phosphate-buffered saline; PLSD, Protected Least Significant Difference; NBT, toluidine *p*-nitrotetrazolium blue; BCIP, 5-bromo-4-chloro-3-indolylphosphate; PB, phosphate buffer; HCL, hair cell layer; SCL, supporting cell layer

* Corresponding author. Tel.: +81 75 751 3346; fax: +81 75 751 7225.
E-mail addresses: kim@ent.kuhp.kyoto-u.ac.jp (T.-S. Kim), tnakagawa@ent.kuhp.kyoto-u.ac.jp (T. Nakagawa).

0378-5955/$ - see front matter © 2005 Elsevier B.V. All rights reserved.
doi:10.1016/j.heares.2005.03.017

There are a number of reports on E-cadherin expression in the inner ear (Whitlon, 1993; Leonova and Raphael, 1997; Whitlon et al., 1999; Hackett et al., 2002; Kim et al., 2002; Simonneau et al., 2003; Kelley, 2003). In damaged inner ear epithelia, supporting cells (SC) surrounding the dying hair cells (HC) rapidly expand and replace the lesion to maintain the barriers that prevent the mixing of endolymph and perilymph, resulting in scar formation (Forge, 1985; Raphael and Altschuler, 1991; Meiteles and Raphael, 1994; Li and Forge, 1995; Steyger et al., 1997; Forge and Li, 2000). In the mammalian cochlea, junctional proteins play a key role in organizing scar formation after aminoglycoside-induced injury (Leonova and Raphael, 1997). In the mammalian vestibular epithelia, our preliminary study (Kim et al., 2002) has indicated that an aminoglycoside, neomycin (NM), which is a potent ototoxic drug, has the potential to transiently alter the expression of adherens junctional proteins including E-cadherin. However, details in changes of cell–cell junctions following aminoglycoside treatment are still fragmentary.

We have previously developed a mouse inner ear damage model using local NM application (Nakagawa et al., 2003). This model induces apoptotic cell death of HC in both cochlear and vestibular epithelia in a well-defined manner. In this study, we examined the relationship between the morphological changes of cell–cell junctions and alterations of E-cadherin expression in damaged vestibular epithelia using this model.

2. Materials and methods

2.1. Animals

C57BL/6 mice aged 10-week-old (SLC, Inc., Hamamatsu, Japan) were used as experimental animals. Experimental protocols and animal care were approved by the Institute of Laboratory Animals Animal Research Committee, Graduate School of Medicine, Kyoto University.

2.2. Experimental groups

In the NM-treated group ($n = 48$), neomycin solution (5 μl; 40% (w/v) in physiological saline; Wako Pure Chemical Industries Ltd, Osaka, Japan) was infused into the perilymphatic space of posterior semicircular canal ducts (PSCC) of the left ear with a microsyringe at a rate of 1 μl/min (Nakagawa et al., 2003), under general anesthesia with ketamine (100 mg/kg, i.p.; Sankyo Pharmaceutical, Tokyo, Japan) and xylazine (9 mg/kg, i.p.; Bayer Japan, Tokyo, Japan). On days 1, 3 and 5 after neomycin treatment, the mice were deeply anesthetized with ketamine and xylazine, and the temporal bones were obtained. Specimens obtained from the right ear, non-treated side, were used as controls. Animals subjected to similar procedures and microinjected with local application of physiological saline (in place of NM) were categorized as the sham-operated group. The temporal bones ($n = 16$) were isolated on day 3 after local application of saline, and the prepared specimens were subjected to statistical analyses for the NM-treated groups.

2.3. Immunohistochemistry

Each animal was perfused intracardially with 0.01 M phosphate-buffered saline (PBS) under deep anesthesia, followed by 4% paraformaldehyde in PBS. The temporal bones were then collected and immersed in the same fixative for 4 h at 4 °C. After rinses with PBS, the utricles were dissected from the temporal bones. Eight utricles from each group were subjected to immunohistochemical analysis in whole-mounts or frozen sections. Following fixation, a portion of the specimens were immersed overnight in PBS containing 30% sucrose before being embedded in OCT compound (Tissue-Tek, Sakura, Tokyo, Japan). Sections (6-μm thickness) were then cut with a cryostat (Leica Microsystems, Tokyo, Japan), and four contiguous sections of each sample at a distance 300 μm from the edge of the vestibular epithelia were provided for histological analysis.

The samples were preincubated with 0.5% Triton X-100 for 30 min at room temperature. After rinsing with PBS, the blocking procedures for immunostaining were performed using a Mouse on Mouse Kit (Vector Laboratories, Burlingame, CA). The samples were then incubated overnight at 4 °C with anti-E-cadherin monoclonal mouse IgG antibodies (×200 dilution; detection site: intracellular lesion, Transduction Laboratories, Lexington, NY), and anti-calretinin polyclonal rabbit IgG antibody (×200 dilution; Chemicon Temecula, CA) to use as a HC marker (Dechesne et al., 1994; Zheng and Gao, 1997; Zheng et al., 1999a; Desai et al., 2005). After rinses with PBS containing 10% goat serum, the samples were incubated for 1 h at room temperature with FITC-conjugated goat anti-mouse IgG2a (×200 dilution; Santa Cruz Biotechnology, Santa Cruz, CA) and goat anti-rabbit IgG-Alexa 546 conjugated (×200 dilution; Molecular Probes, Eugene, OR). After rinses with PBS, the samples were mounted onto glass slides and coverslipped with Vectashield mounting medium (Vector Laboratories). Whole-mount specimens and sections were then viewed with a confocal laser-scanning microscope (TCS-SP2 Leica Microsystems, Tokyo, Japan). In whole-mount specimens, immunolabeling for E-cadherin was examined at 2–4 μm depth below the surface of the sensory epithelia.

2.4. Quantitative assessment of residual HC

Quantification of the number of residual HC was performed by counting the numbers of calretinin-positive cells according to the method reported by Cunningham et al. (2002). A HC density was measured using an eyepiece (10 × 10) reticule. The counting was performed in each of four randomly selected sites of 900 (30 × 30) μm^2 per site in the central region of the utricles. A mean value was determined for each experimental specimen. The HC density of each specimen was expressed as a percentage of the mean value of control specimens. Data was expressed as the mean ± SD.

2.5. Western blot analysis

Four utricles of each experimental group were provided for western blotting for E-cadherin. The samples were homogenized in Laemmli sample buffer (Bio-Rad Laboratories, Hercules, CA). The pellet was treated with 1% β-mercaptoethanol (Bio-Rad Laboratories) before further boiling for 10 min. The total protein concentrations in the samples were determined using an RC DC protein assay (Bio-Rad Laboratories) with a SmartSpec™ 3000 (Bio-Rad Laboratories). Samples containing 10 μg of total protein were loaded onto lanes of 10% polyacrylamide gels (Bio-Rad Laboratories), and proteins were separated by electrophoresis. Protein bands were electrophoretically transferred to PVDF membranes (Millipore, Bedford, MA). Prior to antibody staining, the samples were blocked with 5% skim milk in Tris–PBS buffer (10 mM Tris–HCl, 0.01 M PBS) at pH 8.0 for 1 h. Membranes were then incubated with anti-E- cadherin monoclonal mouse IgG antibodies (×500 dilution; Transduction Laboratories) overnight at 4 °C. Primary antibody binding was detected using biotinylated sheep anti-mouse IgG (×500 dilution; Amersham Biosciences Corp., Piscataway, NJ) for 30 min at room temperature. After rinsing in Tris–PBS, the membranes were incubated with alkaline phosphatase conjugated streptavidin (×3000 dilution; Amersham Biosciences Corp.) in the same incubation buffer for 30 min at room temperature. The blots were then incubated with color-producing substrates; toluidine *p*-nitrotetrazolium blue (NBT) and 5-bromo-4-chloro-3-indolylphosphate (BCIP; Sigma–Aldrich Co., Steinheim, Germany). The apparent molecular masses of labeled bands were determined by comparison with prestained molecular weight protein markers portrayed in adjacent lanes (Bio-Rad). The density of the bands was analyzed quantitatively with NIH image version 1.61 software (Wayne Rasband, National Institutes of Health, Bethesda, MD). The level of expression was defined as the amount relative to that of the control. The analysis was performed four times in each experimental group.

2.6. Transmission electron microscopy

Under deep anesthesia, animals were perfused transcardially with 0.1 M phosphate buffer (PB), followed by 2.5% glutaraldehyde in PB. The temporal bones were immersed in cold fixative for 4 h. Four utricles in each experimental group were isolated in PB and post-fixed in 1% OsO_4 in PB for 2 h on ice. After dehydration in a graded ethanol series, specimens were embedded in Epon-812 and cut into ultra-thin sections. Ultra-thin sections were obtained at 50-μm intervals. The sections were then stained with uranyl acetate and lead citrate, and view with transmission electron microscopy (TEM) (H-7000, Hitachi, Tokyo). A routine photomicrography was performed as follows: A full-frame survey with single-portrayals of the entire sensory epithelium was initially taken at a magnification of ×2000, and then in the apical side of sensory epithelia at higher magnifications (×4000–8000) before evaluation of junctional complexes at much higher magnifications (×10,000–24,000). Junctional complexes were identified by the location of the reticular membrane of SC, which was manifested as a dark band below the apical surface (Engström, 1961; Oesterle et al., 2003).

2.7. Quantitative assessment of degeneration in junctional complexes

We morphologically evaluated 20 junctional complexes in each specimen. TJ and AJ formations between HC and SC, or between adjacent SC were evaluated in the 2.5-fold enlarged photographs in each group. We used the following criteria for estimation of TJ and AJ formations in the junctional complexes: (a) a normal TJ was defined as a cell–cell junction with at least two kissing points, (b) a normal AJ was defined as an intracellular space with extensive condensation of cytoplasmic fibrils along either side of the junctions, and (c) the disruption of each junction was defined as a wider intracellular space. According to these criteria, the numbers of normal TJ and AJ were counted by three authors in a blind manner, and then the percentages of normal TJ and AJ were derived for each specimen. Four utricles were evaluated in each experimental group. Data for each experimental group were expressed as the mean ± SE.

2.8. Statistical analyses

Statistical analysis was performed by one-way ANOVA using Stat View version 5.0 software (SAS Institute, Cary, NC). Individual comparisons were

performed using Fisher's Protected Least Significant Difference (PLSD) for significance ($p < 0.01$) in assessment for HC densities and level of E-cadherin expression, and the Dunnett test in the percentages of assessment for normal TJ and AJ.

3. Results

3.1. Epithelial cell junctions in normal utricles

In control specimens, calretinin immunoreactivity demonstrated the cell bodies of HC (Fig. 1A and B). The expression of E-cadherin was found in the regions corresponding to the cell membranes of HC and SC (Fig. 1A).

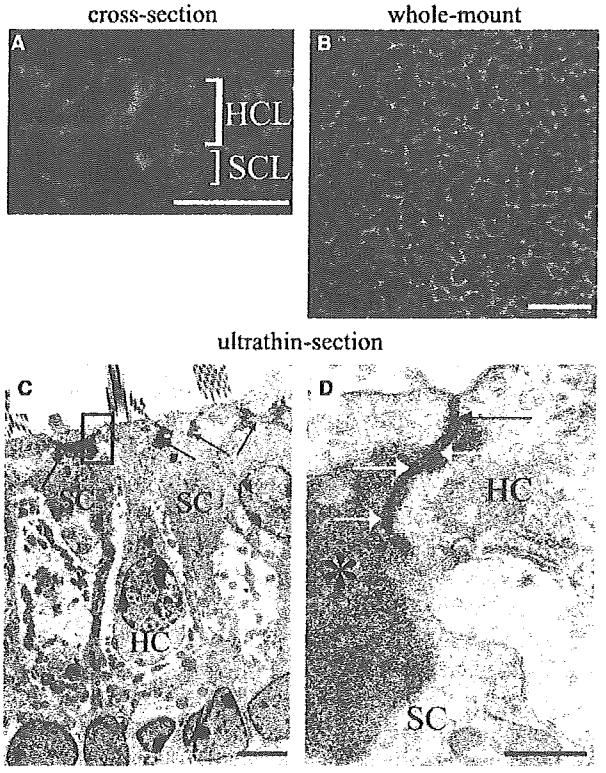

Fig. 1. Expression of E-cadherin and the morphology of junctional complexes in normal vestibular epithelia. A, B: immunostaining for E-cadherin (green) and calretinin (hair cell marker, red); C, D: transmission electron micrographs. E-cadherin expression is found in the regions corresponding to the cell membranes in a cross-section (A, HCL: hair cell layer, SCL: supporting cell layer). The distribution of E-cadherin expression exhibits a honeycomb-like pattern in a whole-mount specimen (B). Immunolabeling for calretinin demonstrates the location of hair cells. Panel D shows a high magnification view of the region indicated by a box in Panel C. HC indicates a hair cell, and SC a supporting cell. Black and white arrows show a tight junction (TJ) and adherens junction (AJ), respectively. The reticular membrane regions are indicated by arrows in Panel C and an asterisk in Panel D. TJ (black arrow) localizes at the apical portion of a junctional complexes. AJ (white arrows) positions just beneath TJ. Bar represents 20 μm (A, B), 4 μm (C) and 500 nm (D), respectively.

In whole-mounts of control specimens, the expression of E-cadherin exhibited a honeycomb-like distribution pattern between HC and SC, or between adjacent SC (Fig. 1B), TEM demonstrated the reticular membrane regions in the apical portion of SC (Fig. 1C). In a high magnifications view, TJ and AJ were identified between HC and SC (Fig. 1D), or between adjacent SC. TJ were located in the upper portions of the lateral cell membranes, and AJ were identified beneath TJ in the level of reticular membrane regions in SC (Fig. 1D).

3.2. E-cadherin expression in damaged utricles

In specimens of the sham-operated group with saline-injected PSCC, immunohistochemistry for calretinin demonstrated numerous surviving HC in sensory epithelia as well as control specimens (Fig. 2A). Quantitative assessment showed no statistically significant difference in HC densities between the control and sham-operated groups (Fig. 3). E-cadherin expression of specimens in the sham-operated group exhibited similar distribution that in the control group in either whole-mounts or frozen sections (Fig. 2A and E). Semi-quantitative analysis by western blotting also demonstrated no significant difference in the level of E-cadherin expression between the control and sham-operated group (Fig. 4). These findings indicated that the procedure for introducing the agents into the PSCC themselves induced no apparent influence on HC survival and E-cadherin expression.

On day 1 after NM treatment, immunostaining for calretinin showed a decrease in HC density (Fig. 2B). HC densities of this group were significantly lower than those of the control or sham-operated groups (Fig. 3). These findings indicated that NM application caused HC deletion from sensory epithelia. Immunoreactivity for E-cadherin became weak, and its distribution was uniform (Fig. 2B and F). Western blot analysis demonstrated a significant decrease of E-cadherin in specimens obtained one day after NM application (Fig. 4). On day 3 after NM application, decrease in HC densities was observed (Fig. 3). Immunoreactivity for E-cadherin on day 3 was weak (Fig. 2C and G), and its distribution was diffuse in sensory epithelia (Fig. 2G). Western blot analysis also demonstrated down-expression of E-cadherin on day 3 (Fig. 4). There were no significant differences in HC densities and levels of E-cadherin expression between day 1 and day 3.

On day 5 after NM application, immunohistochemistry for calretinin demonstrated neither recovery nor further decrease in HC densities (Figs. 2D and 3). While, recovery of immunohistochemistry for E-cadherin was found on day 5. Whole-mount specimens exhibited a honeycomb-like distribution pattern of E-cadherin (Fig. 2E), and E-cadherin expression was observed in the regions corresponding to the cell

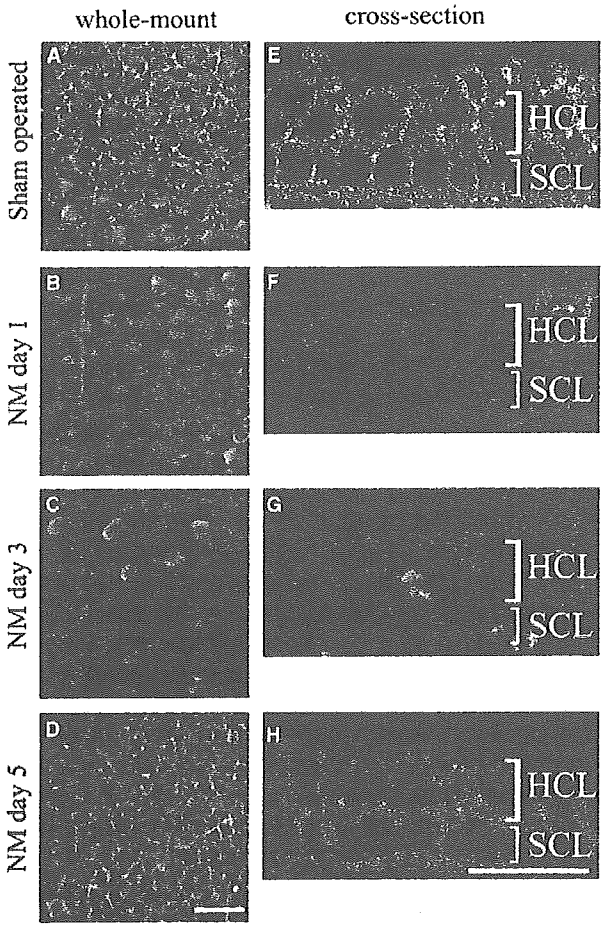

Fig. 2. Alterations of E-cadherin expression in vestibular epithelia following local application of neomycin or physiological saline. A–D: immunostaining for E-cadherin (green) and calretinin (red) in whole-mount specimens; E–H: immunostaining for E-cadherin (green) in cross-sections. HCL indicates a hair cell layer, and SCL a supporting cell layer. In specimens of sham-operated group, which are obtained from animals treated with physiological saline, immunolabeling for calretinin demonstrates a number of hair cells (A). E-cadherin expression distributes in a honeycomb-like pattern (A) and localizes in the regions corresponding to the cell membranes (E). Specimens obtained day 1 after neomycin application (NM day 1) exhibits a weak expression of E-cadherin in a whole-mount (B) and cross-section (F). On day 3 (NM day 3), calretinin-positive cells have decreased and E-cadherin expression is weak (C). E-cadherin expression diffusely distributes within epithelial cells (G). On day 5 (NM day 5), immunostaining for calretinin shows a lower hair cell-density in comparison with that of the sham-operated group (D), while expression patterns of E-cadherin has recovered (D, H) similar to the control. Bar represents 20 μm.

membranes in cross-sections (Fig. 2H). In addition, western blot analysis demonstrated recovery of the level of E-cadherin expression in specimens obtained on day 5 after NM application (Fig. 4). These findings indicated that E-cadherin expression recovered in the amount and distribution pattern on day 5 after NM application, although no recovery of HC densities was noted.

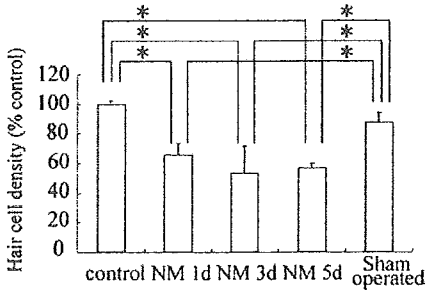

Fig. 3. Alteration in hair cell densities in vestibular epithelia following local application of neomycin or physiological saline. The hair cell density is expressed as a percentage of the control value. Bar represent standard deviations. The differences in hair cell densities between the control and sham-operated groups (treated with physiological saline) are not significant. Hair cell densities of neomycin-treated groups (NM 1d, NM 3d and NM 5d) are significantly lower than those of the control or sham-operated groups (asterisks: $p < 0.01$, ANOVA with Fisher's Protected Least Significant Difference). There are no significant differences among neomycin-treated groups.

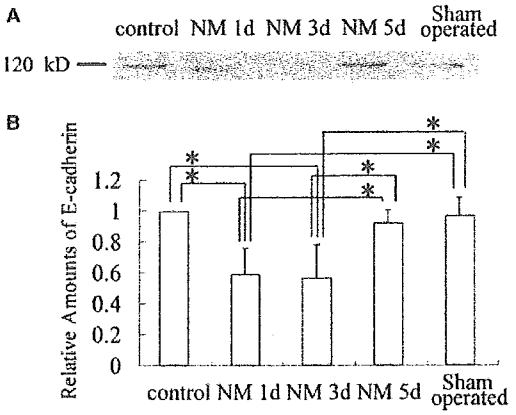

Fig. 4. Western blot analysis for E-cadherin expression in vestibular epithelia following local application of neomycin or physiological saline. A band of E-cadherin in each experimental group is detected as a single band migrating at ca. 120 kDa (A). A mean for an amount of E-cadherin expression relative to the control mean value are presented in Panel B. Each bar represents standard errors. The level of E-cadherin expression on day 1 or day 3 after neomycin treatment (NM 1d, NM 3d) is significantly lower than that of day 5 after neomycin treatment (NM 5d), control or sham-operated specimens (asterisks: $p < 0.01$, ANOVA with Fisher's Protected Least Significant Difference). There are no significant differences among specimens obtained NM 5d, control and sham-operated specimens.

3.3. TEM analysis for junctional complexes

TEM demonstrated details of degeneration of HC and SC, and changes in junctional complexes. In the sham-operated groups, severe degeneration in HC and SC was not observed; however, moderate vacuolization in the cytoplasm of apical portion of HC and SC was found (Fig. 5A). The majority of TJ and AJ between HC and SC (Fig. 5B) or adjacent SC were maintained.

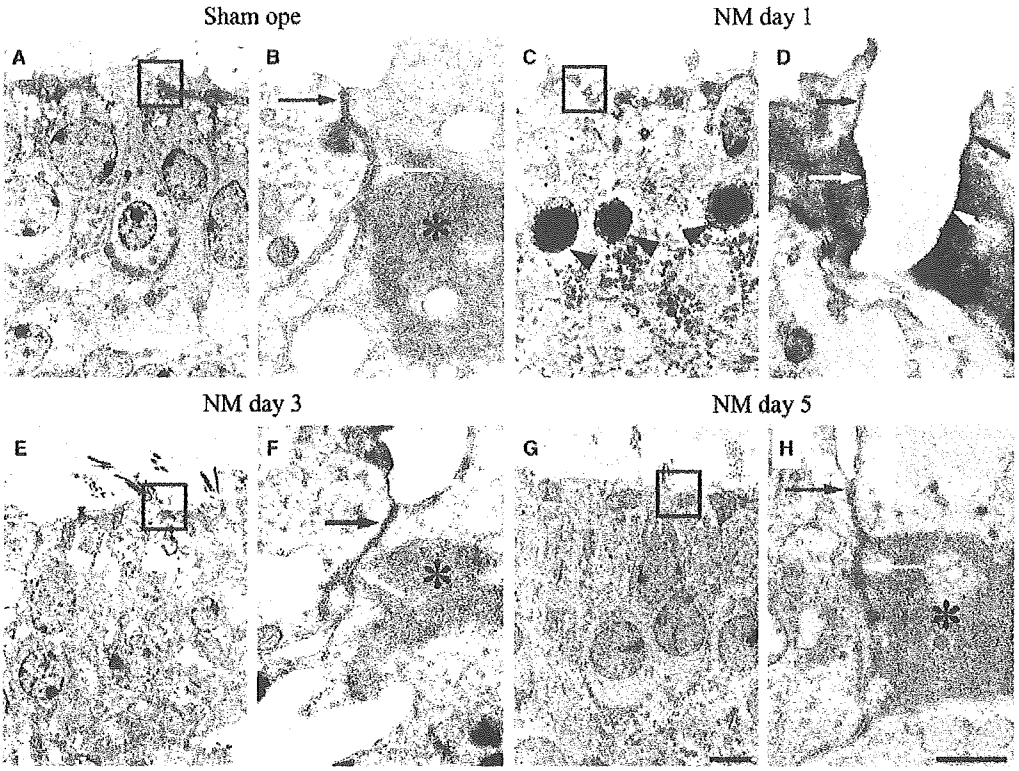

Fig. 5. Transmission electron micrographs of vestibular epithelia following local application of neomycin or physiological saline High magnification images (B, D, F, H) show the region indicated by the boxes in A, C, E and G, respectively. Black and white arrows indicate tight junctions (TJ) and adherens junctions (AJ), respectively. Asterisks show the reticular membrane regions of supporting cells. In specimens treated with physiological saline (sham-operated group), no obvious degeneration is found in epithelial cells and junctional complexes except for blebbing in the cytoplasm (A, B). On day 1 after neomycin treatment (NM day 1), nuclear pyknosis (arrowheads) is frequently observed in hair cells (C). The splitting of TJ and AJ is identified between hair cells and supporting cells (D). On day 3 after neomycin treatment (NM day 3), vacuolization in the cytoplasm is apparent in both hair cells and supporting cells (E), while normal morphology of TJ and AJ between hair cells and supporting cells is identified (F). On day 5 after neomycin treatment (NM day 5), damaged hair cells and supporting cells with blebbing in the cytoplasm were still found (G). The junctional complex exhibits normal morphology (H). Bar represents 4 μm in A, C, E and G, and 500 nm in B, D, F and H.

Quantitative analysis demonstrated no significant differences in TJ or AJ between the control and sham-operated groups (Fig. 6).

On day 1 after NM application, severe degeneration in HC was frequently observed; identical to findings in immunohistochemistry for calretinin. Nuclear pyknosis was frequently found in HC (Fig. 5C). Vacuolization in the cytoplasm was observed in both HC and SC. As for the morphology of junctional complexes, the splitting of TJ and AJ was identified between HC and SC (Fig. 5D) or between adjacent SC, while some TJ and AJ between adjacent SC were maintained. Quantitative analysis demonstrated significant decreases of normal TJ and AJ between HC and SC on day 1 in comparison with the control or sham-operated groups (Fig. 6). However, a trend for decreases in normal TJ and AJ between adjacent SC was observed; however, there were no significant differences in these factors between the control or sham-operated groups and day 1 (Fig. 6).

On day 3 after NM application, vacuolization in the cytoplasm was still observed in both HC and SC (Fig. 5C). Nuclear pyknosis was rarely found in HC. Degeneration of TJ and AJ between HC and SC were still detected; however, normal morphology of TJ and AJ was frequently observed between HC and SC (Fig. 5F). Quantitative analysis demonstrated a trend for decrease of normal TJ and AJ between HC and SC on day 3; however, no significant differences in these factors between the control or the sham-operated groups and day 3 were found (Fig. 6). However, the ratio of normal TJ or AJ between adjacent SC recovered the level of controls (Fig. 6).

On day 5 after NM application, degenerative changes were still observed in HC and SC, albeit the changes subsequently became moderate and approximated those found in the sham-operated group (Fig. 5G). Damaged HC and SC with blebbing in the cytoplasm were observed. The morphology of TJ and AJ between HC and SC (Fig. 5H) or between adjacent SC recovered to the normal state in a manner similar to that in controls. Subsequent quantitative assessments demonstrated no significant differences in the ratio of normal TJ and AJ (Fig. 6).

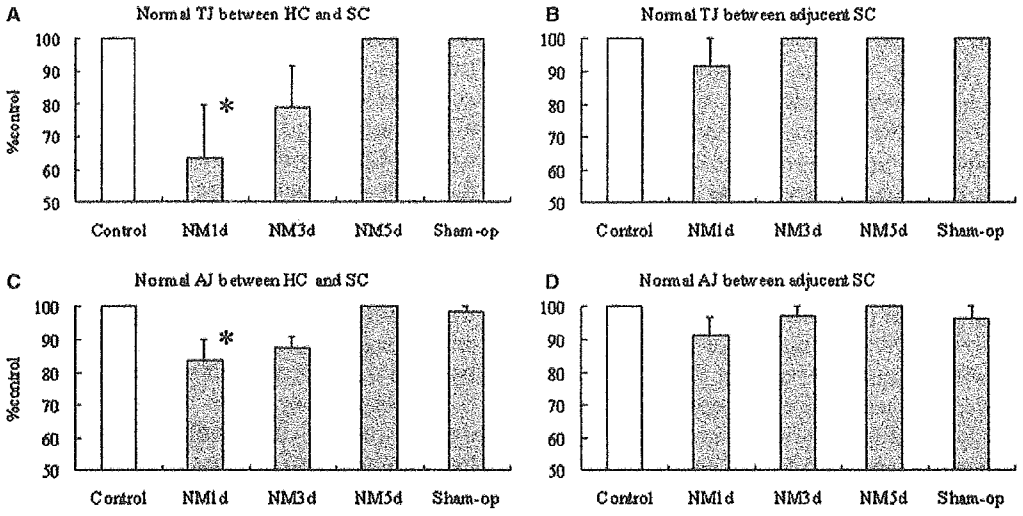

Fig. 6. Quantitative analysis for the ratio of normal tight or adherens junctions in vestibular epithelia following local application of neomycin or physiological saline The ratios of normal tight junctions (TJ) between hair cells (HC) and supporting cells (SC) show in A, those between adjacent supporting cells in B, those of adherens junctions (AJ) between hair cells and supporting cells in C and those between adjacent supporting cells in D. A significant decrease is found in the ratio of normal TJ between HC and SC on day 1 following neomycin treatment (NM 1d) and in that of normal AJ between HC and SC on NM 1d (asterisk in A: $p < 0.05$, ANOVA with Dunnett test).

4. Discussion

Recently, adherens junctional proteins, cadherins and β-catenin, have been paid considerable attention for their role in the regulation of cell proliferation (Nelson and Nusse, 2004). Studies have indicated their crucial role in tumorgenesis and development (Birchmeier and Behrens, 1994; Vleminckx and Kemler, 1999). β-catenin is the central player in the Wnt pathway, and its accumulation in the cytoplasm and following translocation into the nucleus induces transcription of various genes. E-cadherin and β-catenin have been known components of adherens junctions in inner ear sensory epithelia. Alteration in E-cadherin expression has been reported in inner ear sensory epithelia during development (Whitlon et al., 1999). Control of E-cadherin expression can regulate the availability of β-catenin by sequestering it at the cell membrane and thereby rendering it unavailable for signaling to the nucleus (Heasman et al., 1994; Sanson et al., 1996). Based on these findings, we considered that control of E-cadherin expression should be associated with regulation of cell proliferation in inner ear sensory epithelia. Mammalian vestibular epithelia remain a capacity for cell proliferation after birth (Forge et al., 1993; Warchol et al., 1993; Oesterle et al., 2003), although it is very limited (Ogata et al., 1999; Zheng et al., 1999a). Thus, we chose matured mouse vestibular epithelia for evaluation of possible roles of E-cadherin in regulation of cell proliferation after birth. Our preliminary study (Kim et al., 2002) has indicated transient alteration in E-cadherin expression in mouse vestibular epithelia after NM intoxication. However, it has not been examined whether down-expression of E-cadherin actually occurs in vestibular epithelia after injury or not. In addition, details in morphological changes of adherens junctions have not been determined.

In the present study, immunohistochemistry and western blotting demonstrated that down-expression of E-cadherin actually occurred in mouse vestibular epithelia after NM intoxication. We examined E-cadherin expression using an anti-E-cadherin antibody that detects the intracellular regions of E-cadherin. Decreases of E-cadherin expression demonstrated in the present study therefore reflect degradation of cytoplasmic regions of E-cadherin in epithelial cells, which can increase available β-catenin for signaling. We have previously reported a relationship between accumulation of β-catenin and cell proliferation in cultured vestibular epithelia of postnatal day 3 rats (Kim et al., 2004), and in mouse otocysts (Takebayashi et al., 2004). Therefore, down-expression of E-cadherin shown in the present study may be associated with induction of cell proliferation in adult mammalian vestibular epithelia following HC loss. However, the protein level and distribution of E-cadherin expression on day 5 after NM treatment recovered compared to those in the control specimens, which should reduce the availability of β-catenin by sequestering it at the cell membrane. Such immediate recovery of E-cadherin expression may be associated with limited capacity for cell proliferation in mammalian vestibular epithelia.

To examine the relationship between alteration of E-cadherin expression and morphology of cell–cell junctions in vestibular epithelia, we performed TEM

analysis. TEM analysis demonstrated disruption of TJ and AJ between HC and SC, and between adjacent SC. Disruption of TJ and AJ was identified during the period in which down-expression of E-cadherin was observed, indicating close relation between degeneration of epithelial junctions and down-expression of E-cadherin. However, quantitative assessment for TEM findings in TJ and AJ revealed that morphological changes in TJ and AJ were moderate in comparison with the degrees of down-expression of E-cadherin demonstrated by western blotting. On day 1 after NM treatment, the level of E-cadherin expression decreased to 60% of that in the control, while 80% of AJ between HC and SC and 90% of AJ between adjacent SC were kept intact. Therefore, morphology of AJ may maintain even after reduction of E-cadherin expression to 60% of that in the normal condition. In addition, significant decrease of protein levels of E-cadherin expression was observed on days 1 and 3 after NM treatment, while significant losses of normal TJ and AJ between HC and SC was found only on day 1, indicating that morphological disruptions of TJ and AJ were restored prior to the recovery of protein levels of E-cadherin expression. In this study, we used an anti-E-cadherin antibody to detect the intracellular regions of E-cadherin, while TEM analysis focused on morphological changes in extracellular regions of junctional complexes. Such differences may cause a difference in the time course for recovery between morphology of junctional complexes and protein levels of E-cadherin.

Quantitative analysis in TEM findings indicates that disruption of junctional complexes between HC and SC is more frequently observed than that between adjacent SC, which is identical to the vulnerability of HC for aminoglycosides. In the animal model used in this study, deletion of HC in vestibular epithelia through the process of apoptosis predominantly occurs on days 1 and 3 (Nakagawa et al., 2003; Lee et al., 2004). Disruption of junctional complexes and down-expression of E-cadherin also occurred in this period in the present study. Previous studies have demonstrated that there are two modes for deletion of dying HC from sensory epithelia, extrusion from the epithelia and degradation within the epithelia (Li et al., 1995; Nakagawa et al., 1997). Degenerative changes in junctional complexes between HC and SC during the occurrence of HC apoptosis are a rational response for extrusion of dying HC from the epithelium. After deletion of HC, surrounding SC immediately expanded their surfaces to repair the region of HC loss (Forge, 1985; Raphael and Altschuler, 1991; Meiteles and Raphael, 1994; Li and Forge, 1995; Steyger et al., 1997; Forge and Li, 2000), and should form junctional complexes between adjacent SC. We therefore speculate that residual SC may play a central role in the recovery of protein levels of E-cadherin expression.

In contrast to the present findings, no disruptions in the epithelial cell junctions following aminoglycoside treatment have been observed in previous studies (Li et al., 1995; Forge and Li, 2000; Hirose et al., 2004). This may be associated with the difference in drug application routes; local application of aminoglycoside into the inner ear was used in the present study, while previous studies used systemic application. In our model, local application possibly enhances direct effects of NM on cell–cell adhesions in vestibular epithelia. However, further studies of species difference, observation periods and dosages are warranted to clarify the discrepancies between the observations encountered.

In conclusion, local application of NM induced down-expression of E-cadherin and disruption of epithelial cell junctions in mouse vestibular epithelia, and these degenerative changes were rapidly restored. Such rapid recovery of E-cadherin expression may be associated with a limited capacity for cell proliferation in mammalian vestibular epithelia. Recently, it has been reported that some growth factors repress E-cadherin gene transcription (Ciruna and Rossant, 2001; Conacci-Sorrell et al., 2003). These growth factors have effects on the increase of cell proliferation in mammalian vestibular epithelia in vitro (Yamashita and Oesterle, 1995; Zheng et al., 1999b). Therefore, inhibition of reassembly of E-cadherin may increase the activity for cell proliferation in mammalian vestibular epithelia. Further investigations are required for elucidation of the mechanism(s) for regulation of adherens molecules in mammalian vestibular epithelia.

Acknowledgements

We are grateful to J.E. Lee, S. Tamura, M. Fujioka, A. Toyota, T. Tsukamoto and K. Fujita for their technical expertise. We also thank Prof. E.W. Rubel for constructive criticism of the article and Prof. L.E. Westrum and Mr. D.E. Cunningham for helpful comments of TEM analysis. This study was supported by a Grant-in-Aid for Scientific Research (14207068), a Grant-in-Aid for Exploratory Research (15659405) and a Grant-in-Aid for Regenerative Medicine Realization Project from the Ministry of Education, Science, Sports, Culture and Technology of Japan.

References

Birchmeier, W., Behrens, J., 1994. Cadherin expression in carcinomas: role in the formation of cell junctions and the prevention of invasiveness. Biochim. Biophys. Acta 1198, 11–26.

Ciruna, B., Rossant, J., 2001. FGF signaling regulates mesoderm cell fate specification and morphogenetic movement at the primitive streak. Dev. Cell 1, 37–49.

Conacci-Sorrell, M., Simcha, I., Ben-Yedidia, T., Blechman, J., Savagner, P., Ben-Ze'ev, A., 2003. Autoregulation of E-cadherin expres-

sion by cadherin–cadherin interactions: the roles of beta-catenin signaling, Slug, and MAPK. J. Cell Biol. 163, 847–857.
Cunningham, L.L., Cheng, A.G., Rubel, E.W., 2002. Caspase activation in hair cells of the mouse utricle exposed to neomycin. J. Neurosci. 22, 8532–8540.
Dechesne, C.J., Rabejac, D., Desmadryl, G., 1994. Development of calretinin immunoreactivity in the mouse inner ear. J. Comp. Neurol. 346, 517–529.
Desai, S.S., Zeh, C., Lysakowski, A., 2005. Comparative morphology of rodent vestibular periphery. I. Saccular and utricular maculae. J. Neurophysiol. 93, 251–266.
Engström, H., 1961. The innervation of the vestibular sensory cells. Acta Otolaryngol. Suppl. (Stockh) 163, 30–40.
Farquhar, M.G., Palade, G.E., 1963. Junctional complexes in various epithelia. J. Cell Biol. 17, 375–412.
Forge, A., 1985. Outer hair cell loss and supporting cell expansion following chronic gentamicin treatment. Hear. Res. 19, 171–182.
Forge, A., Li, L., Corwin, J.T., Nevill, G., 1993. Ultrastructural evidence for hair cell regeneration in the mammalian inner ear. Science 259, 1616–1619.
Forge, A., Li, L., 2000. Apoptotic death of hair cells in mammalian vestibular sensory epithelia. Hear. Res. 139, 97–115.
Gumbiner, B., Stevenson, B.R., Grimaldi, A., 1988. The role of the cell adhesion molecule uvomorulin in the formation and maintenance of the epithelial junctional complex. J. Cell Biol. 107, 1575–1587.
Hackett, L., Davies, D., Helyer, R., Kennedy, H., Kros, C., Lawlor, P., Rivolta, M.N., Holley, M., 2002. E-cadherin and the differentiation of mammalian vestibular hair cells. Exp. Cell Res. 278, 19–30.
Heasman, J., Crawford, A., Goldstone, K., Garner-Hamrick, P., Gumbiner, B., McCrea, P., Kitner, C., Noro, C.Y., Wylie, C., 1994. Overexpression of cadherins and underexpression of beta-catenin inhibit dorsal mesoderm induction in early Xenopus embryos. Cell 79, 791–803.
Hirose, K., Westrum, L.E., Cunningham, D.E., Rubel, E.W., 2004. Electron microscopy of degenerative changes in the chick basilar papilla after gentamicin exposure. J. Comp. Neurol. 470, 164–180.
Kelley, M.W., 2003. Cell adhesion molecules during inner ear and hair cell development, including notch and its ligands. Curr. Top. Dev. Biol. 57, 321–356.
Kim, T.S., Nakagawa, T., Endo, T., Iguchi, F., Murai, N., Naito, Y., Ito, J., 2002. Alteration of E-cadherin and beta-catenin in mouse vestibular epithelia during induction of apoptosis. Neurosci. Lett. 329, 173–176.
Kim, T.S., Nakagawa, T., Lee, J.E., Fujino, K., Iguchi, F., Endo, T., Naito, Y., Omori, K., Lefebvre, P.P., Ito, J., 2004. Induction of cell proliferation and beta-catenin expression in rat utricles in vitro. Acta Otolaryngol. Suppl. 551, 22–25.
Lee, J.E., Nakagawa, T., Kim, T.S., Iguchi, F., Endo, T., Kita, T., Murai, N., Naito, Y., Lee, S.H., Ito, J, 2004. Signaling pathway for apoptosis of vestibular hair cells of mice due to aminoglycosides. Acta Otolaryngol. Suppl. 551, 69–74.
Leonova, E.V., Raphael, Y., 1997. Organization of the cell junctions and cytoskeleton in the reticular lamina in normal and ototoxically damaged organ of Corti. Hear. Res. 113, 14–28.
Li, L., Forge, A., 1995. Cultured explants of the vestibular sensory epithelia from adult guinea pigs and effects of gentamicin: a model for examination of hair cell loss and epithelial repair mechanisms. Audit. Neurosci. 1, 111–125.
Li, L., Nevill, G., Forge, A., 1995. Two modes of hair cell loss from the vestibular sensory epithelia of the guinea pig inner ear. J. Comp. Neurol. 355, 405–417.
Meiteles, L., Raphael, Y., 1994. Scar formation in the vestibular sensory epithelium after aminoglycoside toxicity. Hear. Res. 79, 26–38.
Nakagawa, T., Yamane, H., Shibata, S., Takayama, M., Sunami, K., Nakai, Y., 1997. Two modes of auditory hair cell loss following acoustic overstimulation in the avian inner ear. O.R.L. J. Otorhinolaryngol. Relat. Spec. 59, 303–310.
Nakagawa, T., Kim, T.S., Murai, N., Endo, T., Iguchi, F., Tateya, I., Yamamoto, N., Naito, Y., Ito, J., 2003. A novel technique for inducing local inner ear damage. Hear. Res. 176, 122–127.
Nelson, W.J., Nusse, R., 2004. Convergence of Wnt, beta-catenin, and cadherin pathways. Science 303, 1483–1487.
Oesterle, E.C., Cunningham, D.E., Westrum, L.E., Rubel, E.W., 2003. Ultrastructural analysis of [3H]thymidine-labeled cells in the rat utricular macula. J. Comp. Neurol. 18, 177–195.
Ogata, Y., Slepecky, N.B., Takahashi, M., 1999. Study of the gerbil utricular macula following treatment with gentamicin, by use of bromodeoxyuridine and calmodulin immunohistochemical labelling. Hear. Res. 133, 53–60.
Raphael, Y., Altschuler, R.A., 1991. Reorganization of cytoskeletal and junctional proteins during cochlear hair cell degeneration. Cell Motil. Cytoskel. 18, 215–227.
Sanson, B., White, P., Vincent, J.P., 1996. Uncoupling cadherin-based adhesion from wingless signalling in Drosophila. Nature 383, 627–630.
Simonneau, L., Gallego, M., Pujol, R., 2003. Comparative expression patterns of T-, N-, E-cadherins, beta-catenin, and polysialic acid neural cell adhesion molecule in rat cochlea during development: implications for the nature of Kolliker's organ. J. Comp. Neurol. 459, 113–126.
Steyger, P.S., Burton, M., Hawkins, J.R., Schuff, N.R., Baird, R.A., 1997. Calbindin and parvalbumin are early markers of non-mitotically regenerating hair cells in the bullfrog vestibular otolith organs. Int. J. Dev. Neurosci. 15, 417–432.
Takebayashi, S., Nakagawa, T., Kojima, K., Kim, T.S., Kita, T., Endo, T., Iguchi, F., Yamamoto, N., Naito, Y., Ito, J., 2004. Beta-catenin distribution in the developing cochlea of mice. A.R.O. abstract.
Takeichi, M., 1991. Cadherin cell adhesion receptors as a morphogenetic regulator. Science 251, 1451–1455.
Tsukita, Sh., Tsukita, Sa., Nagafuchi, A., Yonemura, S., 1992. Molecular linkage between cadherins and actin filaments in cell–cell adherens junctions. Curr. Opin. Cell Biol. 4, 834–839.
Vleminckx, K., Kemler, R., 1999. Cadherins and tissue formation: integrating adhesion and signaling. Bioessays 21, 211–220.
Warchol, M.E., Lambert, P.R., Goldstein, B.J., Forge, A., Corwin, J.T., 1993. Regenerative proliferation in inner ear sensory epithelia from adult guinea pigs and humans. Science 259, 1619–1622.
Whitlon, D.S., 1993. E-cadherin in the mature and developing organ of Corti of the mouse. J. Neurocytol. 22, 1030–1038.
Whitlon, D.S., Zhang, X., Pecelunas, K., Greiner, M.A., 1999. A temporospatial map of adhesive molecules in the organ of Corti of the mouse cochlea. J. Neurocytol. 28, 955–968.
Yamashita, H., Oesterle, E.C., 1995. Induction of cell proliferation in mammalian inner-ear sensory epithelia by transforming growth factor alpha and epidermal growth factor. Proc. Natl. Acad. Sci. USA 92, 3152–3155.
Zheng, J.L., Gao, W.-Q., 1997. Analysis of rat vestibular hair cell development and regeneration using calretinin as an early marker. J. Neurosci. 17, 8270–8282.
Zheng, J.L., Keller, G., Gao, W.-Q., 1999a. Immunocytochemical and morphological evidence for intracellular self-repair as an important contributor to mammalian hair cell recovery. J. Neurosci. 19, 2161–2170.
Zheng, J.L., Frantz, G., Lewis, A.K., Sliwkowski, M., Gao, W.-Q., 1999b. Heregulin enhances regenerative proliferation in postnatal rat utricular sensory epithelium after ototoxic damage. J. Neurocytol. 28, 901–912.

The Laryngoscope
Lippincott Williams & Wilkins, Inc.

Drug Delivery to the Cochlea Using PLGA Nanoparticles

Tetsuya Tamura, MD; Tomoko Kita, PhD; Takayuki Nakagawa, MD, PhD; Tsuyoshi Endo, MD; Tae-Soo Kim, MD, PhD; Tsutomu Ishihara, PhD; Yutaka Mizushima, MD, PhD; Megumu Higaki, MD, PhD; Juichi Ito, MD, PhD

Objectives: **This study aimed to investigate the efficacy of encapsulating therapeutic molecules in poly lactic/glycolic acid (PLGA) nanoparticles for drug delivery to the cochlea.** ***Study Design:*** **An experimental study.** ***Methods:*** **We examined the distribution of rhodamine, a fluorescent dye, in the cochlea, liver, and kidney of guinea pigs. Intravenous injection of rhodamine or rhodamine-encapsulated PLGA nanoparticles was used to target the fluorescent dye systemically to the liver, kidney, and cochlea, and these molecules were applied locally to the round window membrane (RWM) of the cochlea. The localization of rhodamine fluorescence in each region was quantitatively analyzed.** ***Results:*** **After systemic application of rhodamine nanoparticles, fluorescence was identified in the liver, kidney, and cochlea. The systemic application of nanoparticles had a significant effect on targeted and sustained delivery of rhodamine to the liver but not the kidney or cochlea. Rhodamine nanoparticles placed on the RWM were identified in the scala tympani as nanoparticles, indicating that the PLGA nanoparticles can permeate through the RWM. Furthermore, the local application of rhodamine nanoparticles to the RWM was more effective in targeted delivery to the cochlea than systemic application.** ***Conclusions:*** **These findings indicate that PLGA nanoparticles can be an useful drug carrier to the cochlea via local application.** ***Key Words:*** **Drug delivery, nanoparticle, cochlea, inner ear, rhodamine.**
Laryngoscope, **115:2000–2005, 2005**

From the Department of Otolaryngology-Head and Neck Surgery, Kyoto University Graduate School of Medicine, Kyoto, Japan (T.T., T.K., T.N., T.E., T.-S.K., J.I.); the DDS Institute, The Jikei University School of Medicine, Tokyo, Japan (T.I., Y.M.); and the Institute of Medical Science, St Marianna University School of Medicine, Kawasaki, Japan (Y.M., M.H.).

Editor's Note: This Manuscript was accepted for publication July 20, 2005.

This study was supported by a Grant-in-Aid for Regenerative Medicine Realization from the Ministry of Education, Science, Sports, Culture and Technology of Japan.

Corresponding author: Takayuki Nakagawa, MD, PhD, Department of Otolaryngology-Head and Neck Surgery, Graduate School of Medicine, Kyoto University, Kawaharacho 54, Shogoin, Sakyo-ku, 606-8507 Kyoto, Japan. E-mail: tnakagawa@ent.kuhp.kyoto-u.ac.jp

DOI: 10.1097/01.mlg.0000180174.81036.5a

INTRODUCTION

The advancement of inner ear medicine will require the development of a means of nontraumatic and nontoxic delivery of therapeutic molecules to the cochlea. However, drug delivery to the cochlea presents a number of technical challenges, which have hindered the development of therapeutic strategies for the treatment of sensorineural hearing loss and related inner ear disorders. Reasons for the difficulty of drug delivery to the cochlea include the limited blood flow to the cochlea[1] and the existence of the blood-labyrinth barrier, which limits the transportation of molecules from blood to cochlear tissues.[2] The sustained delivery of therapeutic molecules is also critical for the efficient treatment of the cochlea, because bioactive molecules usually require a period of minutes or hours over which to produce their pharmacological actions. Consequently, a number of researchers are currently working to solve these problems and develop methods for the local application of molecules into the cochlea.[3,4]

Encapsulating bioactive molecules in nanoparticles consisting of biodegradable polymers such as poly-lactic/glycolic acid (PLGA) enables the sustained release of bioactive molecules in a controlled manner.[5] Recent advances in this field have made it possible to prepare PLGA nanoparticles using relatively simple techniques.[6] The present study aimed to examine the potential of PLGA nanoparticles for use as a vehicle for systemic and local drug delivery to the cochlea. We prepared PLGA nanoparticles encapsulating rhodamine, a red fluorescent dye, and administered these systemically or locally to adult guinea pigs. The profiles of rhodamine delivery to the cochlea were then analyzed using histologic techniques.

MATERIALS AND METHODS

Preparation of Rhodamine Nanoparticles

A PLGA formulation with a lactic/glycolic acid ratio of 50/50 was purchased from Wako Pure Chemicals Industries, Ltd. (Osaka, Japan). PLGA nanoparticles were prepared by an oil-in-water solvent diffusion method described elsewhere.[5] Briefly, a mixture of 20 μL of 0.5 mol/L zinc acetate aqueous solution and 0.7 mL of acetone dissolved in 20 mg of PLGA (Mw 8000) and 1 mg of rhodamine B (Sigma Chemical Co., St. Louis, MO) was added to 5 mL of a 0.5% (w/v) egg yolk lecithin (Sigma) aqueous

suspension. To chelate the zinc, 1 mL of 0.5 mol/L EDTA aqueous solution (pH 7.5) was added to the resulting suspension of nanoparticles. The nanoparticles were purified from unencapsulated rhodamine by ultrafiltration (YM-50, Millipore Co., Bilenica, MA) and subsequent gel filtration (PD-10 column, Amersham Biosciences, Tokyo, Japan). The diameter of the nanoparticles ranged from 140 to 180 nm.

Animals

Pigmented guinea pigs weighing 250 to 300 g were purchased from Japan SLC Inc. (Hamamatsu, Japan) for use in this study. The Animal Research Committee, Graduate School of Medicine, Kyoto University approved all experimental protocols, and animal care was supervised by the Institute of Laboratory Animals, Graduate School of Medicine, Kyoto University. All experimental procedures were performed in accordance with National Institutes of Health (NIH) guidelines for the care and use of laboratory animals.

Systemic Application

Experimental animals were anesthetized with ketamine (20 mg/kg IM; Sankyo Co., Tokyo, Japan) and xylazine (5 mg/kg IM; Bayer, Tokyo, Japan). We exposed the right femoral vein and injected PLGA nanoparticles encapsulating rhodamine B (nanoRho; 0.25 mL, 20 μg/mL physiological saline) into 12 animals and normal, unencapsulated rhodamine B (Rho; 0.25 mL, 20 μg/mL physiological saline) into eight animals. At 10 or 120 minutes after injection of rhodamine, the animals were killed by cervical rotation under anesthesia with a lethal dose of ketamine and xylazine. The left temporal bones, kidney, and liver were immediately excised from the animals. The cochleae were dissected in cold 0.01-mol/L phosphate-buffered saline at pH 7.4 (PBS), and the kidney and liver were cut into approximately 1 cm^3 blocks. The specimens were immersed in 10% trichloroacetic acid in PBS at 4°C for 24 hours. After washing with PBS, specimens were embedded in OCT compound (Tissue-Tek, Sakura Finetechnical, Tokyo, Japan) and frozen at −80°C until use.

Local Application

Under general anesthesia with ketamine and xylazine, the bulla of the left temporal bone was exposed using a retroauricular approach. A small hole was made on the bulla to expose the round window membrane (RWM). A piece of gelfoam immersed with nanoRho (0.25 mL, 20 μg/mL physiological saline) was placed on the RWM of four animals. The same amounts of unencapsulated Rho were applied to another four animals. The cochleae were then collected 24 hours after application. Tissue preparation was performed according to the procedure described above for samples from systemically treated animals. To examine the dynamics of these molecules in the cochlea, we used a glass pipette to inject 10 μL of nanoRho through the RWM into the scala tympani of three animals, at the same concentration as that placed on the RWM. The temporal bones were collected 24 hours after the injection and used for histologic analysis.

Analysis of Rhodamine Distribution

Tissue specimens were cut into 10-μm thick sections. Four mid-modiolus sections from the cochleae of each animal were used for histological analysis. The specimens were covered with Vector Shield (Vector Laboratories Inc., Burlingame, CA), and viewed with a Nikon ECLIPSE E600 fluorescence microscope (Nikon, Tokyo, Japan). We counted the number of red fluorescent rhodamine particles within the cochlea in every section and calculated the mean number of particles from four sections, for each animal, for statistical analyses.

Four randomly selected sections from the liver and kidney of each animal were also used for histologic analysis. The numbers of rhodamine particles in five random fields of 0.4 mm^2 were counted in each section. The mean number of rhodamine particles from the four sections was determined for each animal.

Statistics

We calculated the differences in the numbers of red fluorescent particles between nanoRho and Rho at 10 or 120 minutes after systemic application. The Mann-Whitney U test was used for all statistical calculations, and a probability (P) value of less than 0.05 was considered to be significant. Values are expressed as mean ± SE.

RESULTS

Liver and Kidney

In the liver, rhodamine fluorescence was found in every experimental group (Fig. 1). Rhodamine fluorescence was observed as moderate red fluorescent dots following application of Rho (Fig. 1C), and as intense red fluorescent dots following nanoRho application (Fig. 1A, B). A number of red fluorescent dots were observed at 10 minutes after Rho application (74.5 ± 4.5), but this figure had decreased significantly to 8.5 ± 0.6 at 120 minutes (P = 0.0008, Fig. 2A). Numerous red fluorescent dots were found in the liver after nanoRho application: 542.4 ± 61.2 at 10 minutes and 533.8 ± 24.8 at 120 minutes (Fig. 2A). There was no significant difference in numbers of red fluorescent dots between these two time points, indicating that the PLGA nanoparticles promoted sustained delivery of rhodamine to the liver. The application of nanoRho resulted in significantly higher numbers of red fluorescent dots in the liver than were seen after Rho application, at 10 (P = 0.0002) and 120 minutes (P = 0.0002) after application (Fig. 2A), showing that PLGA nanoparticles are significantly more effective at targeting delivery of Rho to the liver.

In the kidney, few or no red fluorescent dots were identified after application of Rho (10 min: 0.3 ± 0.3, 120 min: 0; Fig. 1D, 2B) or nanoRho (10 min: 4.4 ± 2.0, 120 min: 0.2 ± 0.2; Fig. 2B). There was no significant difference in the number of red fluorescent dots in the kidney between 10 and 120 minutes for either Rho or nanoRho application, or between these two preparations of Rho. These findings indicate that PLGA nanoparticles have no significant impact on the effectiveness of targeted delivery of rhodamine to the kidney.

Cochleae after Systemic Application

In the cochlea, no red fluorescent dots were observed after systemic application of Rho, whereas they were observed after systemic application of nanoRho (Fig. 1E-H). Rhodamine particles were localized in spiral prominence (Fig. 1E), stria vascularis (Fig. 1F), or the cochlear melodious (Fig. 1G, H). The regions in which rhodamine particles were localized corresponded to the location of blood vessels in the cochlea. Rhodamine fluorescence was found in the apical, middle, and basal portion of the cochlea. The number of red fluorescent dots after nanoRho application was 2.8 ± 0.3 at 10 minutes and 0.1 ± 0.1 at 120 minutes (Fig. 2C), and the difference between 10 and 120 minutes was significant at $P < 0.0001$. The numbers of rhodamine